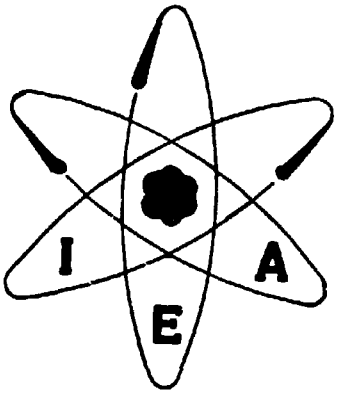

REFLECTIVITY OF A Ge NEUTRON CRYSTAL MONOCHROMATOR AND THE IEA-R1 REACTOR SPECTRUM MEASUREMENT

R. FULFARO

PUBLICAÇÃO IEA N.º 243
Julho — 1971

INSTITUTO DE ENERGIA ATÔMICA
Caixa Postal 11049 (Pinheiros)
CIDADE UNIVERSITARIA "ARMANDO DE SALLES OLIVEIRA"
SAO PAULO — BRASIL

REFLECTIVITY OF a Ge NEUTRON CRYSTAL MONOCHROMATOR AND THE IEA-R1 REACTOR SPECTRUM MEASUREMENT

R. Fulfaro

Divisão de Física Nuclear
Instituto de Energia Atômica
São Paulo - Brasil

Publicação IEA Nº 243
Julho - 1971

Comissão Nacional de Energia Nuclear

Presidente: Prof.Dr. Hervásio Guimarães de Carvalho

Universidade de São Paulo

Reitor: Prof.Dr. Miguel Reale

Instituto de Energia Atômica

Diretor: Prof.Dr. Rômulo Ribeiro Pieroni

Conselho Técnico-Científico do IEA

Prof.Dr. José Moura Gonçalves
Prof.Dr. José Augusto Martins
Prof.Dr. Rui Ribeiro Franco — pela USP
Prof.Dr. Theodoreto H.I. de Arruda Souto — pela CNEN

Divisões Didático-Científicas

Divisão de Física Nuclear -
Chefe: Prof.Dr. José Goldenberg

Divisão de Radioquímica -
Chefe: Prof.Dr. Fausto Walter de Lima

Divisão de Radiobiologia -
Chefe: Prof.Dr. Rômulo Ribeiro Pieroni

Divisão de Metalurgia Nuclear -
Chefe: Prof.Dr. Tharcísio D.S. Santos

Divisão de Engenharia Química -
Chefe: Lic. Alcídio Abrão

Divisão de Engenharia Nuclear -
Chefe: Engº Pedro Bento de Camargo

Divisão de Operação e Manutenção de Reatores -
Chefe: Engº Azor Camargo Penteado Filho

Divisão de Física de Reatores -
Chefe: Prof.Dr. Paulo Saraiva de Toledo

Divisão de Ensino e Formação -
Chefe: Prof.Dr. Rui Ribeiro Franco

Divisão de Física do Estado Sólido -
Chefe: Prof.Dr. Shigueo Watanabe

REFLECTIVITY OF a Ge NEUTRON CRYSTAL MONOCHROMATOR AND THE IEA-R1 REACTOR SPECTRUM MEASUREMENT

R. Fulfaro

ABSTRACT

The thermal neutron spectrum of the IEA-R1 reactor has been measured in the wavelength interval from 0.3 Å to 3.0 Å, using a neutron crystal spectrometer. A Germanium single crystal in reflection was used as monochromator because the second order reflections from its (111) planes are theoretically forbidden.

The Germanium crystal reflectivity employed in the analysis of the data was calculated for the first five permited orders. An effective absorption coefficient of the crystal was used to perform the calculations instead of the macroscopic cross section of the element used in calculations performed by other authors.

The spectrum count rate has been corrected for higher order contamination and parasitic reflections and processed in order to obtain the effective thermal neutron spectrum as a function of wavelength.

A Maxwellian equation type was adjusted by least squares fit to the experimental points between 0.7 Å and 2.9 Å. The experimental results are compared with a theoretical Maxwellian distribution and the effective neutron temperature was found to be $351 \pm 8^{\circ}K$ which is $45^{\circ}K$ above the average moderator temperature of $306^{\circ}K$.

I. INTRODUCTION

The neutrons that reach thermal equilibrium with the moderator nuclei after loosing energy during the moderation process in a nuclear reactor are called thermal neutrons.

This class of neutrons presents a velocity distribution approximately Maxwellian[1], where the kinetic energy that corresponds to the most probable velocity, at an absolute temperature T, is given by $\frac{1}{2} m v_t^2 = kT$; m is the neutron mass and k the Boltzmann constant. It is very useful for experimental purpose to have an expression that describes the spectral distribution of neutrons emerging from a reactor beam hole. This distribution is

particularly interesting for the technique of absolute flux standardization by activation of foils detectors[2].

In general, with thermal neutron experiences, spectrometers are required in order to select the neutrons by their energies.

The present work describes the method employed in the measurement of reactor spectra with a single crystal neutron spectrometer.

This type of instrument is often used, since in a comparison with other types of spectrometers, presents some advantages, such as: good stability of calibration and resolution, and the advantage of producing an intense continuous beam of monochromatic neutrons. These characteristics make the crystal spectrometer particularly suitable for precise measurements at specific energies.

The principle of the spectrometer operation is based on the selective diffraction from a single crystal, which is governed by the Bragg equation.

(1) $$\lambda = (2d \sin\theta)/n \quad \text{with} \quad n = 1, 2, 3, \ldots$$

where n is the order of reflection, λ is the neutron wavelength, d is the spacing of the crystal appropriate planes and θ is the glancing angle of the neutron beam with these planes. Variations of θ produce corresponding variations of λ, and hence of the neutron energy.

The source of neutrons for this work was the Instituto de Energia Atômica swimming pool research reactor operated at 2 MW. In a general way, the crystal spectrometer, constructed at the IEA workshop, is similar to what has been described in the

literature[3,4]. A schematic diagram of the IEA neutron crystal spectrometer is shown in figure 1.

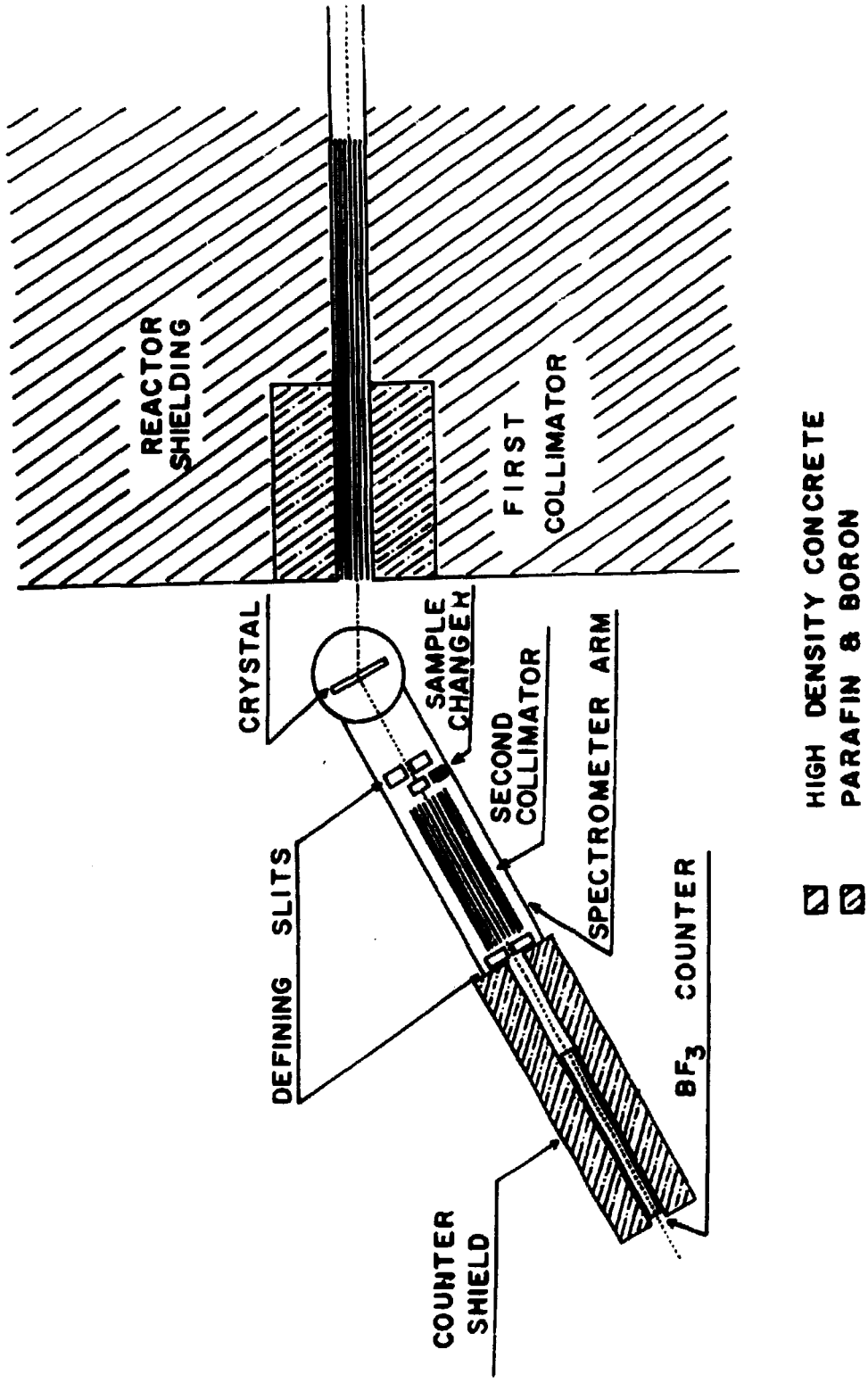

Figure 1 - Schematic diagram of the IEA neutron crystal spectrometer

The polyenergetic neutron beam emerging from a beam hole reactor passes through the first collimator, is diffracted by the crystal, then passes through the second collimator and is detected by a boron trifluoride proportional counter placed at the end of the spectrometer arm.

For each wavelength, i.e., fixed θ angle, the measured count rate will be a function of collimation, crystal reflectivity, detector efficiency and spectral distribution of neutrons emerging from the reactor.

Therefore, in order to obtain the thermal neutron distribution from the count rate measurements, it is necessary to calculate the crystal reflectivity, taking into account experimental resolution, and to calculate the detector efficiency. It is also necessary to correct the experimental data from higher order contamination and parasitic reflections effects.

II. CRYSTAL REFLECTIVITY

Before presenting the crystal reflectivity calculation equations, it is interesting to make some considerations about the nature of the crystals used as neutron monochromators. These crystals are composed of "mosaic blocks" of the order of 5000 Å across which, although individually perfect, are separated from each other by dislocations and hence not in a perfect alignment.

The "mosaic blocks" angular distribution is normally assumed to have a Gaussian shape, i.e.[5],

$$W(\Delta) = (1/\eta\sqrt{2\pi}) \exp - (\Delta^2/2\eta^2) \qquad (2)$$

Here $\eta = \beta/2\sqrt{2\ln 2}$, and the "mosaic spread" β is the full width at half maximum of the distribution.[9] In eq.(2), W is defined so that $W(\Delta).d\Delta$ is the fraction of mosaic blocks having

their normals between the angles Δ and $\Delta+d\Delta$ to the normal to the surface crystal.

Suitable monochromating crystals usually are of the type called "ideally imperfect", where the individual mosaic blocks are assumed small enough and therefore "primary extinction" can be ignored, i.e., the beam attenuation due to a perfectly ordered structure does not occur in the block; only the "secondary extinction" is considered, i.e., the beam attenuation by Bragg scattering from identically oriented mosaic blocks.

In crystals of that type the actual intensity variation inside the crystal is approximated by a smoothed curve, for which a differential equation can be set up and solved.[6]

Crystal reflectivity expressions had been deduced by some authors[6,7,8]. The present work deals with the case of reflection by an ideally imperfect crystal fixed at its Bragg position in a collimated beam of polyenergetic radiation. The solution of the coupled differential equations describing the behaviour of the incident and diffracted beam in traversing a layer dt of a crystal of total thickness t_o, is given by

$$(3) \qquad R^{\theta} = cte \int I_1(\delta_1)\ P(\theta,\Delta)\ I_2(\delta_2)\, d\Delta$$

where $I_1(\delta_1)$ and $I_2(\delta_2)$ are the acceptance functions of the collimators. These functions can, in a good approximation, be considered as having Gaussian forms[9] with halfwidths equal to the angular divergences α_i of the collimators:

$$(4) \qquad I_i(\delta_i) = \frac{1}{\alpha_i' \sqrt{2\pi}} \exp\left[-\frac{\delta_i^2}{2\alpha_i'^2}\right]$$

with $\alpha_i' = \alpha_i / 2\sqrt{2 \ln 2}$ and δ being the angular divergence from

the central passage through the collimator. In the case of different angular divergences, $\alpha_1 \neq \alpha_2$, it is enough to substitute α_i by $\alpha_e/\sqrt{2}$ with $\alpha_e = \sqrt{\alpha_1^2 + \alpha_2^2}$ and the same equations (3) and (4) can be used[15].

In eq. (3) it is necessary to evaluate the constant in order to determine absolute intensities[9]. However, when dealing with crystal reflectivity the constant need not to be considered[6].

$P(\theta,\Delta)$ represents the reflectivity of the mosaic blocks with an angular displacement Δ from the average orientation, for the neutrons characterized by a Bragg angle θ, and is given by

$$P(\theta,\Delta) = \frac{a}{(1+a) + \sqrt{1+2a}\ \coth\left[A\sqrt{1+2a}\right]} \tag{5}$$

with

$$A = \frac{\mu t_o}{\gamma_o}$$

$$a = \left(\frac{Q}{\mu}\right) W(\Delta) \tag{6}$$

where μ is the effective absorption coefficient and γ_o is the sine of the mean Bragg angle.

The crystallographic quantity Q, is given by

$$Q = (\lambda^3 N_c^2/\sin 2\theta)\ F^2 \tag{7}$$

where N_c is the number of unit cells per unit volume, F is the structure factor, which is given as

$$F_{hkl}^2 = \left| \sum b\, e^{-2M}\ \exp 2\pi Ni(hx_i + ky_i + lz_i) \right|^2 . \tag{8}$$

The summation is taken over all atoms in the unit cell, b being the nuclear scattering amplitude. The Debye Waller temperature correction factor e^{-2M}, originated from the thermal vibrations of the atoms, was discussed and justified by several authors[10,11]. The analytical expression for M used in the calculations is

$$M = \frac{6\,h^2}{m\,k\,\Theta}\left(\frac{n}{2d}\right)^2\left[\frac{1}{4} + \left(\frac{T}{\Theta}\right)^2 \cdot \Lambda\left(\frac{\Theta}{T}\right)\right] \tag{9}$$

Here, Θ is the crystal Debye temperature, h and k are Planck's and Boltzmann's constants, respectively, m is the nuclear mass, d is the grating space, and n is the order number. The Debye function $\Lambda(\frac{\Theta}{T})$ is given by[11]

$$\Lambda(z) = \int_0^z \frac{x}{e^x - 1}\,dx \tag{10}$$

T being the crystal temperature in degrees Kelvin.

In equations (6), the effective absorption coefficient μ represents the crystal total macroscopic cross section, but without considering the elastic coherent scattering by the monochromating planes. It is given by[13]

$$\mu = N\left\{\sigma_a + \sigma_i + \sigma_c\left[1 - (1 - e^{-\tau})/\tau\right]\right\} \tag{11}$$

where N is the number of atoms per cm^3 of the crystal, σ_a is the capture microscopic cross section, σ_i is the incoherent microscopic scattering cross section of a single nucleus, and $\sigma_c = 4\pi\,b^2$ is the coherent nuclear cross section.

τ is given by

$$(12) \qquad \tau = \left(\frac{24\ E\ m'}{k\ \Theta\ m}\right) \left[\frac{1}{4} + \left(\frac{T}{\Theta}\right)^2 \cdot \Lambda\left(\frac{\Theta}{T}\right)\right]$$

where all symbols, except the energy E and the mass m' of neutron, were defined earlier for eq. (9). In figure 2 the results of eq. (11) are plotted for a Germanium single crystal over the wavelength range 0.3 to 3.5 Å[13].

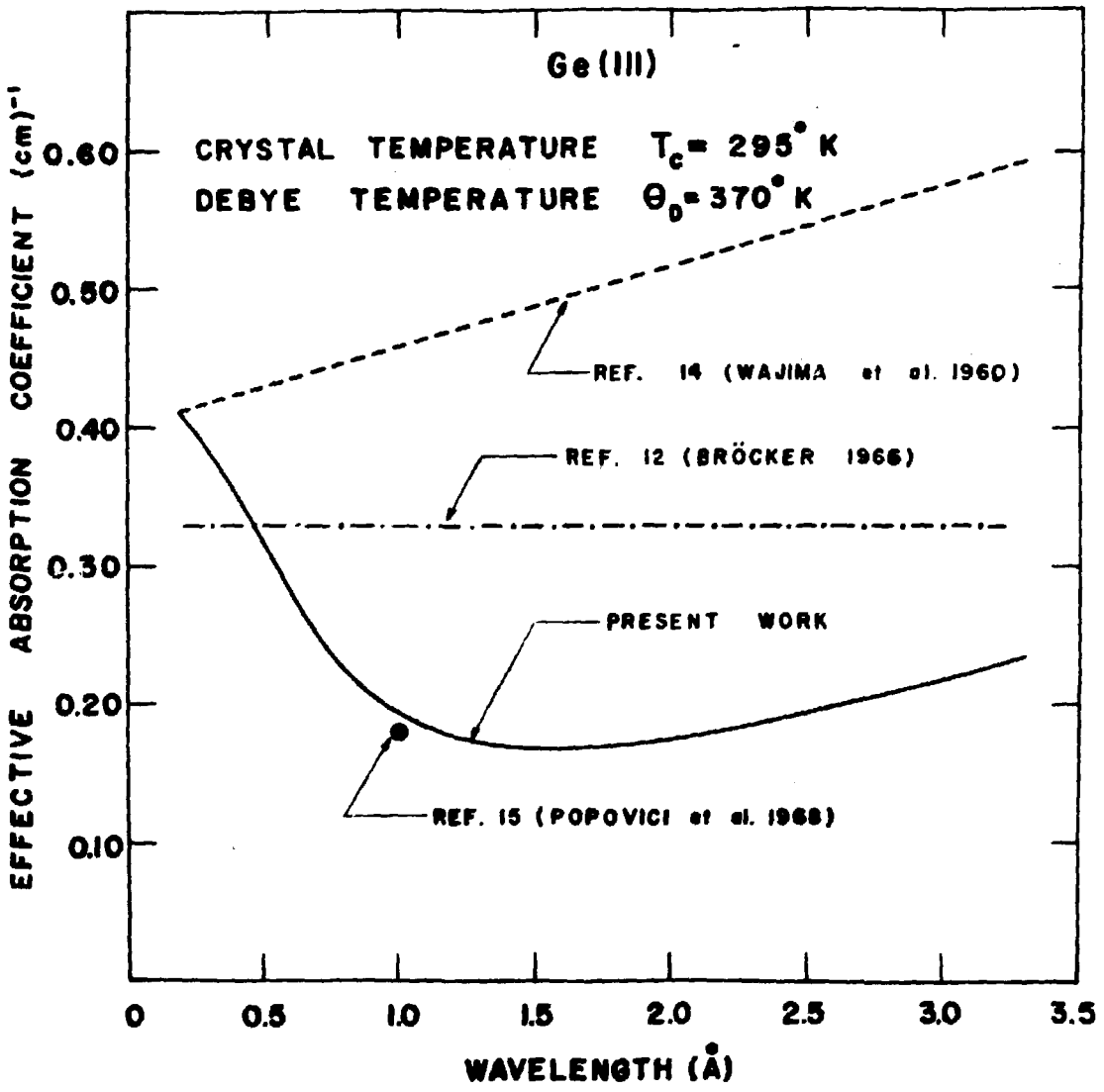

Figure 2 - Effective absorption coefficient of Germanium single crystal

For the effective absorption coefficient of a Ge crystal, calculations were previously made by other investigators[12,14]. However, the total macroscopic cross section of the element was used instead of the crystal cross section. Wajima et al.[14] used $\mu = N(\sigma_a + \sigma_s)$ and Bröcker[12] used a constant value $\mu=0.33\ cm^{-1}$. In fact, only Popovici[15] in 1968 calculated the Ge crystal effective absorption coefficient, but only for the wavelength $\lambda=1.0\text{Å}$ and the obtained value $\mu = 0.18\ cm^{-1}$ agrees with the results of the present work at this same wavelength.

The R^θ reflectivity calculation as defined by eq. (3) can be made using the set of equations (4) to (12). The R^θ has the following physical interpretation: it is the angular range over which reflection can be considered complete.

However, an angular interval $\Delta\theta$ is related to a wavelength interval $\Delta\lambda$ by the derivative of the Bragg equation

$$\Delta\lambda = 2d \cos\theta \ \Delta\theta/n \tag{13}$$

Hence, a R^λ can be associated to R^θ and one can write[16]

$$R^\lambda = R^\theta \ (2d \cos\theta/n) \tag{14}$$

In this value of R^λ are included the crystal reflectivity or the efficiency of reflection at a given wavelength, and the instrument resolution function, that is the wavelength interval in which reflection occurs.

Therefore, if $\phi(\lambda)$ is the flux per unit wavelength interval per unit area and time, the number of neutrons reaching the detector each second is $\phi\ (\lambda)\ R^\lambda$. If $\varepsilon\ (\lambda)$ is the detector efficiency, then the experimentally observed count rate $I(\lambda)$ will be proportional to $\phi(\lambda)R^\lambda\ \varepsilon(\lambda)$. Thus, except for a constant, one can write

(15) $$I(\lambda) = \phi(\lambda) R^{\lambda} \varepsilon(\lambda)$$

HIGHER ORDER CONTAMINATIONS

Higher order contaminations are always present in the diffraction process which produce the Bragg reflections, since any neutrons satisfying the equation (1), i.e., $n\lambda = 2 d \sin\theta$ can be reflected. The value n = 1 is the first-order reflection which corresponds to neutrons of the desired wavelength λ, while the values n = 2,3,... give the undesirable higher order contamination. Hence, the reflected neutron beam consists of neutrons with wavelength λ and a contamination of neutrons with wavelengths $\lambda/2$, $\lambda/3$, ... etc.

At wavelengths above the peak of the thermal spectrum, order contaminations can be serious, since the flux at $\lambda/2$ or $\lambda/3$ may be comparable or even considerably larger than the flux at the primary wavelength λ. Hence, when a measurement is made at longer wavelengths, additional terms must be added to the right-hand side of eq. (15) for higher order contributions to the count rate. The measured count rate $I(\lambda)$ thus becomes.

(16) $$I(\lambda) = \sum_{n=1}^{m} \phi(\lambda/n) R^{\lambda n} \varepsilon(\lambda/n)$$

where the upper limit m of summation will depend on the desirable accuracy and the part of the spectrum being measured.

Higher order reflections are repressed relatively to the first order reflection, by several factors. Observing fig. 2, one can see that the effective absorption coefficient tends to discriminate against shorter wavelength neutrons compared to those of longer wavelength. The R^{θ} as function of n is reduced through the factor Q, defined by eq. (7), by a factor of n^3 because it is a function of λ^3. The Debye Waller factor, eqs. (8) and (9), con

tributes to hold the higher order as a function of n; and finally in eq.(14) an additional factor of 1/n is introduced in the transformation of R^{θ} to R^{λ}.

A program was written for the IEA-IBM1620 computer to carry out calculation of the crystal reflectivity $R^{\theta n}$ for all orders of reflections. The program termed REFLETI can be used for any monochromating crystal in reflection, as well as any set of diffracting planes, mosaic spread, crystal thickness and collimator divergence.

In figure 3, the reflectivity $R^{\theta n}$ for the (111) set of

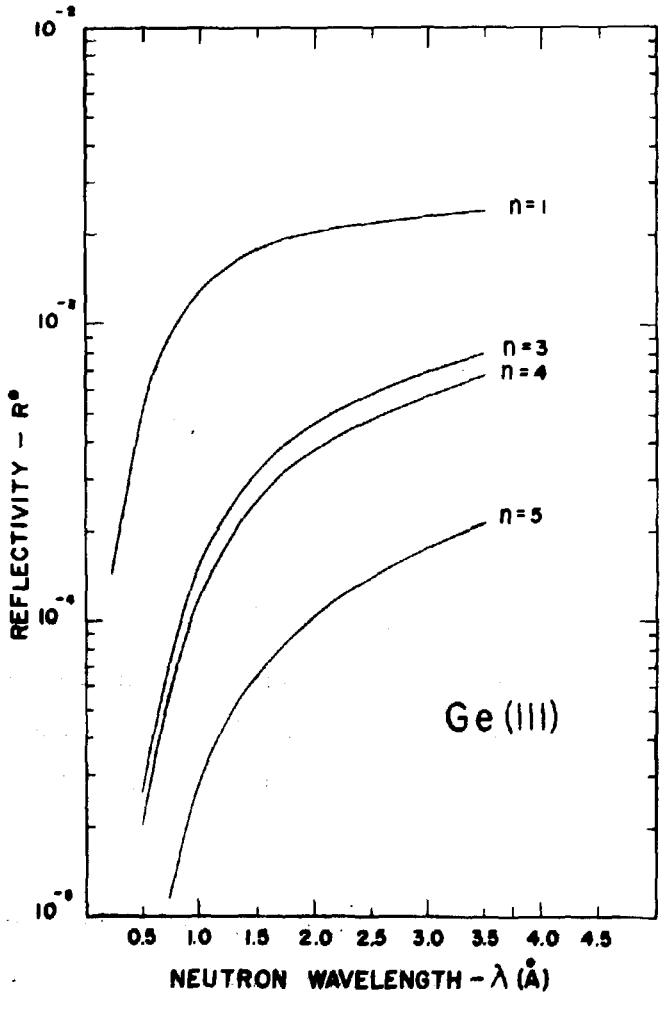

Figure 3 - Reflectivity R^{θ} for the (111) set of planes of a Germanium single crystal, used in reflection, for the n values 1, 3, 4, 5.

planes of a Germanium single crystal is plotted for n=1,3,4 and 5. The second order reflectivity was not calculated because it is theoretically forbidden for the Ge(111). In X-ray and neutron diffraction a crystal reflection is called "forbidden" when the structure factor of the unit cell is zero. In this case the interference among the waves scattered by the atoms of the unit cell gives a resulting wave of zero amplitude.

For the diamond like lattice (Germanium case), the f.c.c. reflections of the form $h + k + 1 = 4\nu + 2$ ($\nu = 0,1,2,...$) have zero structure factor: $F^2_{(hkl)} \equiv 32b^2$ for $(h + k + 1) = 4\nu \pm 1$ and $F^2_{(hkl)} \equiv 64b^2$ for $(h + k + 1) = 4\nu$.

The calculation of the curves in fig. 3 was performed using these rules for F^2 and the values[16]: $b = 0.84 \times 10^{-12}$ cm, $N_c = 5.55 \times 10^{22}$ cm^{-3}, $\Theta = 370^{\circ}$K and $T_c = 295^{\circ}$K.

DETECTOR EFFICIENCY

For a neutron beam incident axially upon an enriched, high pressure BF_3, the detector efficiency is given by[17]

$$(17) \qquad \varepsilon = \exp - (n_1\sigma_1 t_1 + n_2\sigma_2 t_2) \left[1 - \exp(-n_2\sigma_2 t_3) \right]$$

where $n_1\sigma_1$ is the macroscopic absorption cross section of the window material, t_1 is the window thickness, n_2 is the number of B^{10} atoms/cm^3, σ_2 is the cross section of B^{10}, t_2 is the length of the inactive region at the window end, and t_3 is the active length of the detector.

In the experiments to be described, the neutron beam diffracted by the crystal is detected by a proportional counter, filled to a pressure of 60 cm, enriched to 96% in the B^{10} isotope.

The detector is a Nancy Wood Co. model with 1-in diameter, and having $t_1 = 0.135$ cm of aluminum, $t_2 = 1.75$ cm and $t_3 = 50.8$ cm. For this detector $n_1\sigma_1 t_1$ is negligible compared to $n_2\sigma_2 t_2$.

The detector efficiency calculation as a function of energy was made by the eq. (18), using the value 3838 barns for σ_2 at the thermal energy (0.0253 eV)[18]. A plot of detector efficiency from 0.001 eV to 1.0 eV is shown in figure 4. The inactive length effect is seen to dominate the detector performance at low energies.

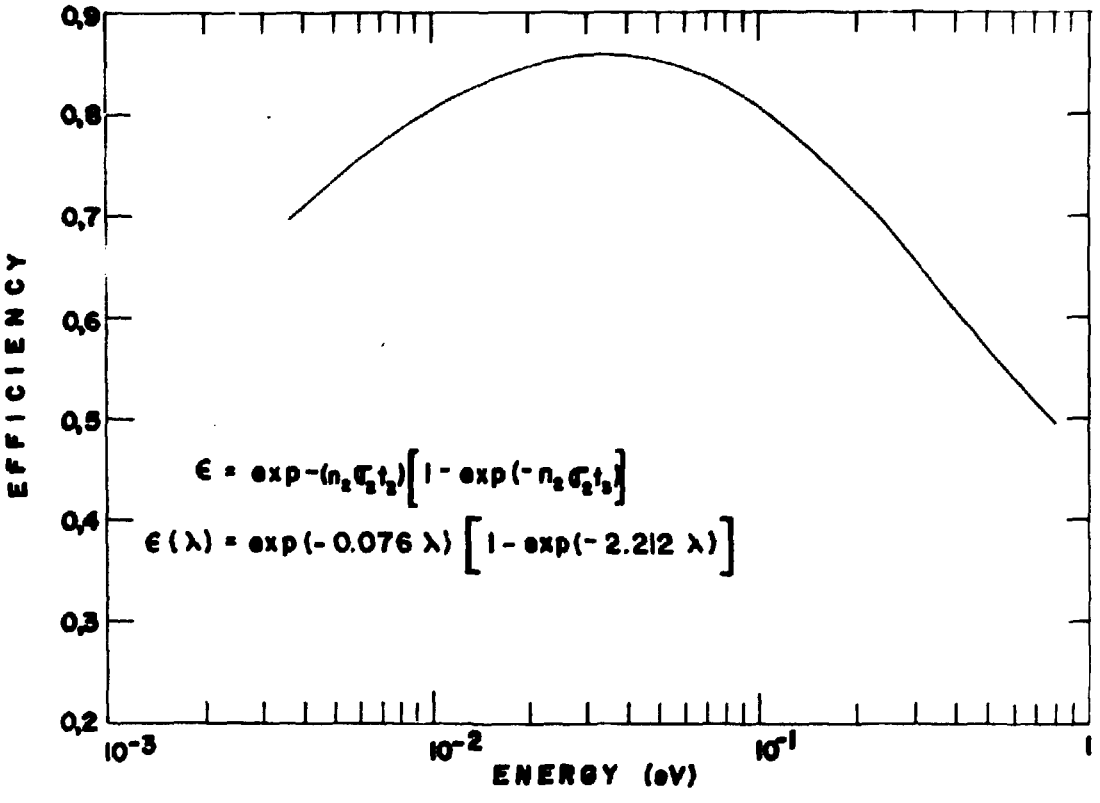

Figure 4 - Detector efficiency versus neutron energy

PARASITIC REFLECTIONS

The measured count rate curve with a crystal monochromator as function of wavelength, contains flutuations in form of inverted peaks identified as effects of parasitic reflections.

A parasitic reflection occurs when crystal planes, other than the plane being used to obtain the monochromatic beam, also simultaneously satisfies the Bragg conditions for a given wavelength. Neutron reflection by more than one crystal plane in a single crystal happens when the sphere of reflection intersects more than one lattice point in reciprocal lattice[5].

The parasitic reflections problem was intensively studied because of their complicating effects on reactor spectrum measurement with a crystal spectrometer[19,20,21]. In order to eliminate the parasitic reflections effects it is enough to rotate the monochromating crystal about an axis perpendicular to the reflecting plane[19,22]. By this procedure, the permanence of other point of reciprocal lattice in the sphere of reflection is avoided.

After the rotation over this azimuthal angle, a new experimental point of the count rate is obtained, giving a continuous sequence to a point joining the inverted peak that have been existed in the curve. In the present work the parasitic reflection problem was avoided by this procedure.

III. MEASUREMENT OF THE IEA-R1 REACTOR SPECTRUM

The thermal neutron spectrum measurement was made using a Germanium single crystal having a disc shape (7.62cm dia x 1.51cm) with the (111) planes parallel to the face. The crystal was grown by the Semi Elements Inc. of Saxonburg, Pennsylvania. The interplanar spacing of Ge(111) is $d_{111} = 3.2603$ Å.

Germanium crystals are commonly used as monochromators because the second order reflections from its (111) planes are theoretically forbidden.

The rocking curve of the crystal, shown in figure 5, is

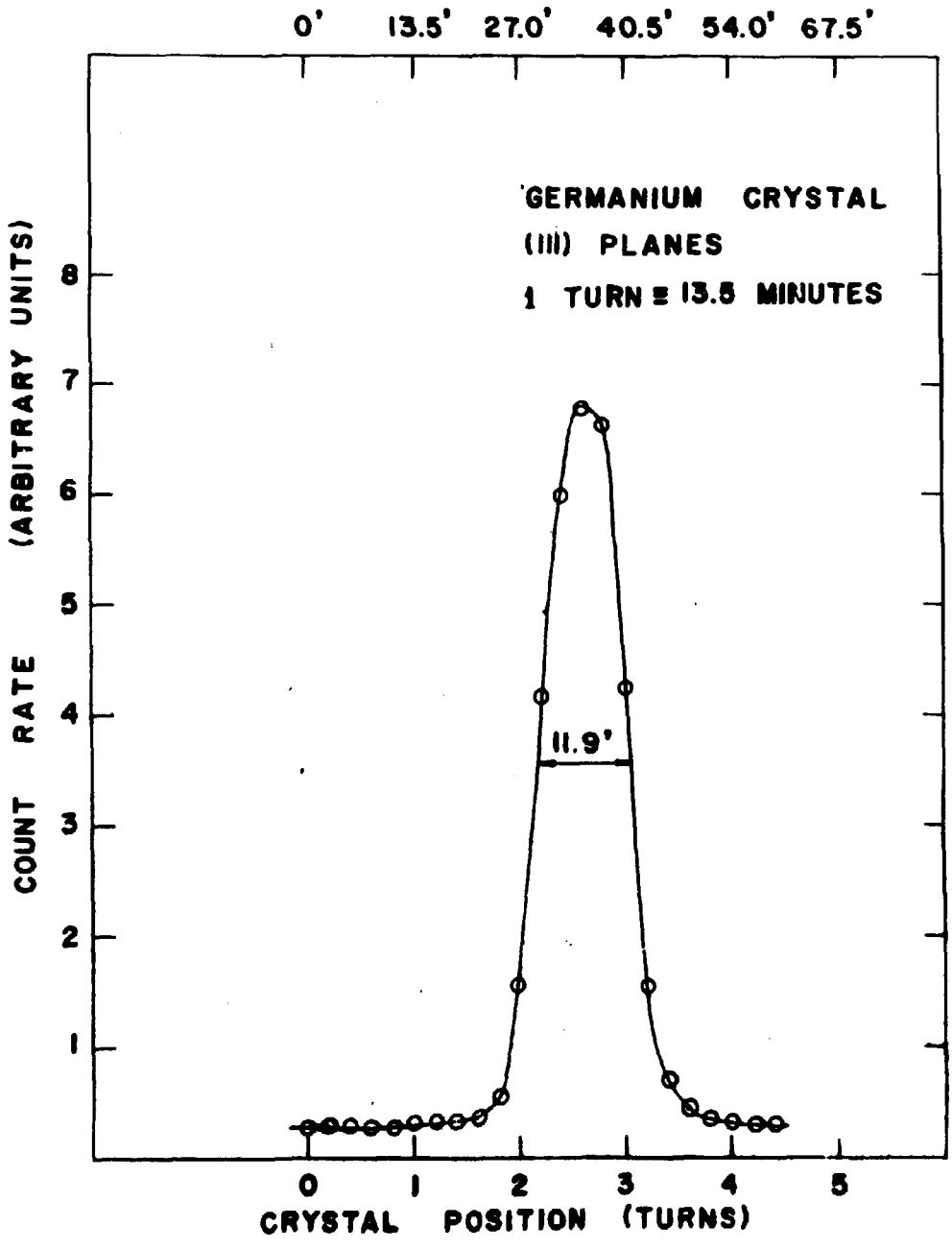

Figure 5 - Rocking curve for Germanium crystal in reflection. Peak counting rate is approximately 1.2 x 10^4 counts/min.

obtained holding the spectrometer arm stationary and rotating the crystal about its Bragg position. The utility of this curve is to put the crystal in the position of maximum diffracted intensity for a given Bragg angle, and also to obtain the mosaic spread β, from the full width at half-maximum W of the rocking curve.

A expression describing the rocking curve for a mosaic single crystal, can be approximated by a normal distribution with a standard deviation[15]

$$W' = \sqrt{(\alpha'/2)^2 + \eta^2} \tag{19}$$

where α' and η were previously defined.

The angular divergences of the first and the second collimators, used with the IEA crystal spectrometer, are α_1=15.16 min and α_2=14.72 min, respectively. Hence α_e = 21.13 min and the mosaic spread, determined from $W = 2W' \sqrt{2\ell n 2}$, is β = 5.47 min . The experimental β value is a parameter which enters directly into calculation of the crystal reflectivity R^{θ} as given by eq.(3).

COUNT RATE MEASUREMENT AND THE THERMAL SPECTRUM DETERMINATION

Figure 6 shows the observed count rate for neutrons reflected from the (111) planes of a Germanium crystal as a function of neutron wavelength. In order to avoid changes in reactor power, the counting time for these measures were taken for a preset number of monitor counts.

In figure 6, mainly on the 1.2 to 1.4 Å interval, the inverted peaks due to the parasitic reflections can be noted, and in this interval it is difficult to ascertain what experimental points are free from their perturbing influence.

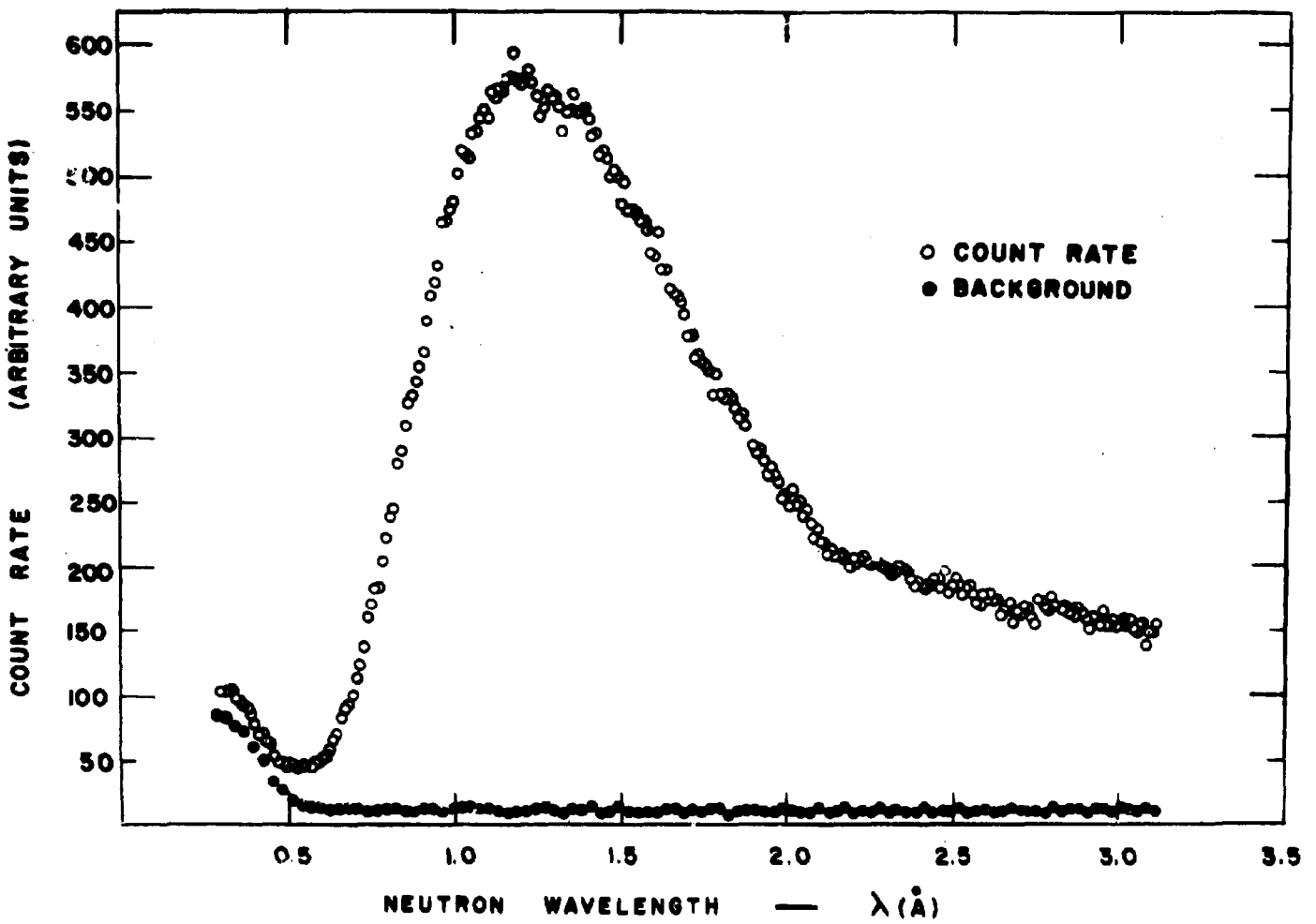

Figure 6 - Count rate measured using a Ge(111) crystal in reflection

However, the parasitic planes which produce these depressions in figure 6, are not parallel to the primary Bragg planes (111) of the crystal face. Hence, the Bragg angles at which given parasitic reflections occur and also their corresponding inteusities, can be changed by rotating the crystal about the axis perpendicular to the face. This fact permits to obtain enough points free of parasitic reflections to determine the unperturbed count rate curve with reasonable accuracy[22].

In figure 7 the experimental points obtained by the above procedure and corrected for background, are described by the curve termed I, in the 0.3 to 3.0 Å wavelenth interval. The background was determined by turning the crystal 2 degrees from its Bragg position about the vertical rock axis.

The higher order contribution to the count rate is negligible in the short wavelength range, such as for λ smaller than the thermal spectrum peak wavelength. Thus, eq. (16) can be rewritten as

$$I(\lambda) = \sum_{n=1}^{m} I_n \tag{20}$$

where,

$$I_n = \phi(\lambda/n) R^{\lambda n} \varepsilon(\lambda/n) \tag{21}$$

In the lower region of the 0.3 to 3.0 Å wavelength interval, a good approximation for the I curve in figure 7 is to make $I(\lambda) \equiv I_1(\lambda)$.

In fact, the calculated $I_3(\lambda)$ even at 1.0 Å is smaller than 0.5% of the observed count rate and does not exceed 1% of $I(\lambda)$ till 1.5 Å .

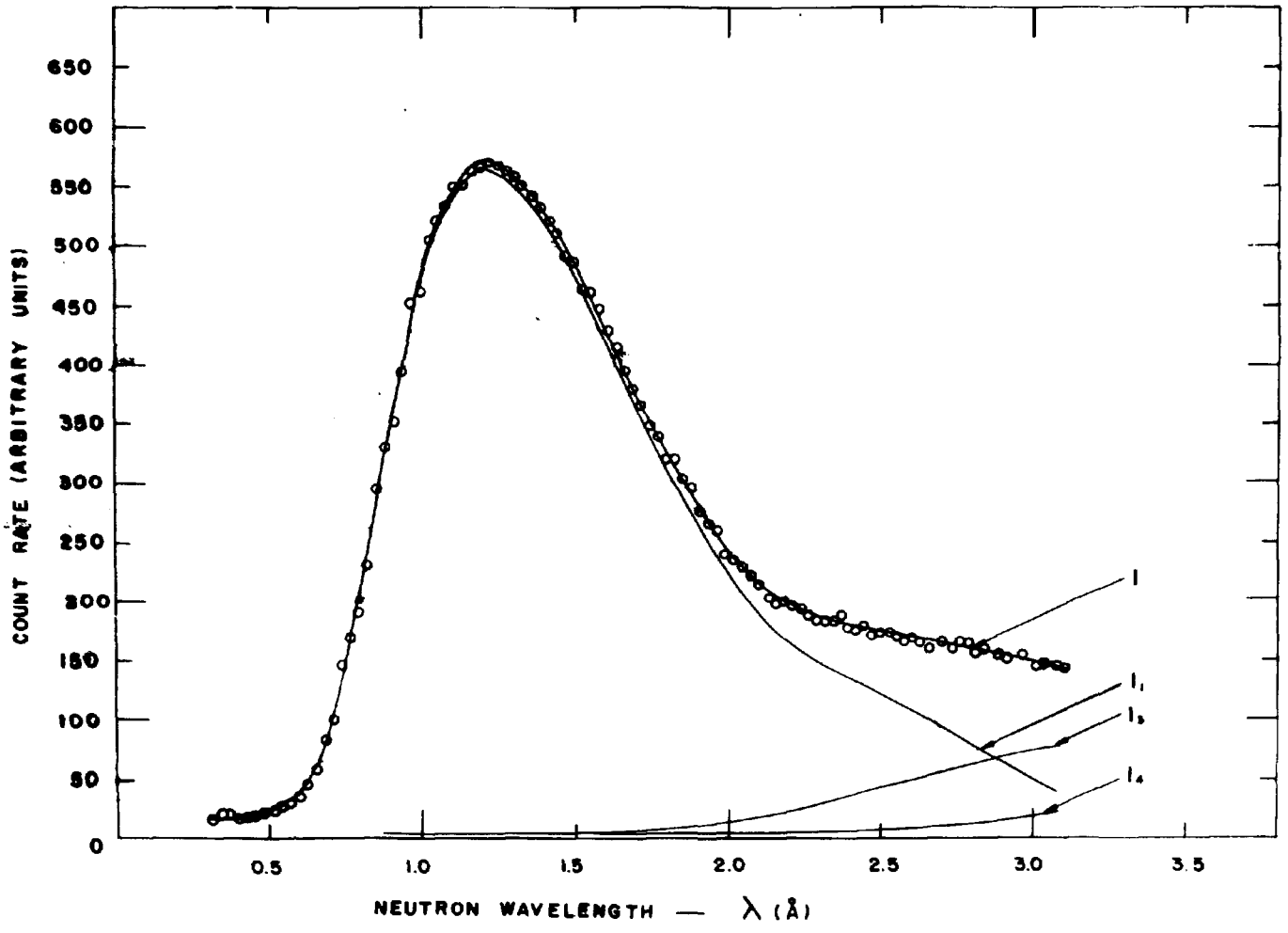

Figure 7 - Count rate for Ge(111) crystal corrected for background and effects of parasitic reflections

At 3.0 Å, the upper end of the wavelength range considered, the $\lambda/3$ belongs to the region where the contamination is negligible. Hence, the fluxes $\phi(\lambda/n)$ can be experimentally determined at a given λ, by means of a count rate measurement at λ/n.

$$\phi(\lambda/n) = \frac{I(\lambda/n)}{R^{(\lambda/n)1}\ \varepsilon(\lambda/n)} \tag{22}$$

where $R^{(\lambda/n)1}$ is the first order reflectivity at the λ/n wavelength.

Using the equations (22) and (23) gives

$$I_n(\lambda) = I(\lambda/n)\ \frac{R^{\lambda n}}{R^{(\lambda/n)1}} \tag{23}$$

where $R^{\lambda n}$ is the reflectivity of order n, at the wavelength λ.

The higher order intensities allowed for the (111) planes of the Germanium crystal were individually calculated and are plotted together with the curve I in figure 7 as a function of neutron wavelength.

The neutron flux per unit wavelength interval was calculated from the first order intensity (fig. 7), using the equation $\phi(\lambda) = I_1(\lambda)/R^{\lambda}\ \varepsilon(\lambda)$. The experimental point of the resultant $\phi(\lambda)$ are plotted versus wavelength in figure 8.

IV. DISCUSSION OF RESULTS

A thermal neutron flux spectrum can be approximatelly described by a Maxwellian distribution having the form[1]

$$\phi(\lambda) = 2N(E/kT)^2 \left[\exp\ (-E/kT)\right]/\lambda \tag{24}$$

where $\phi(\lambda)\, d\lambda$ is the number of neutrons emerging per second in the wavelength range between λ and $\lambda + d\lambda$, N is the total neutron flux of all energies, E the energy corresponding to the wavelength λ, k the Boltzmann's constant and T(^{o}K) characteristic temperature of the distribution.

However, the thermal neutron spectrum emerging from a beam hole reactor is never exactly a Maxwellian corresponding to the moderator temperature.

The real thermal neutron distribution is shifted to a higher energy and the corresponding effective temperature is higher than the moderator temperature. Among the effects which tend to shift the spectrum one can mention the incomplete moderation in the available moderator between the fuel elements and the initial beam hole surface; neutrons which are still being slowed down contributing to a 1/E spectrum; and absorbing atoms in the moderator with absorption cross section having $1/\sqrt{E}$ energy dependence.

Hence, a Maxwellian equation type, i.e., $\phi(\lambda) = K\, \lambda^{-M} \exp\left[-(\lambda_o/\lambda)^2\right]$, was adjusted to the experimental flux points between 0.7 to 2.9 Å. A program for the IEA computer was used to perform the parameters choice by least squares fit, and the resulting equation is given by

$$\phi(\lambda) = 101.883\, \lambda^{-4.61} \exp\left[-(1.644/\lambda)^2\right] \qquad (25)$$

Figure 8 shows the calculated curve, eq.(25), describing perfectly the experimental flux points at the considered wavelength interval. Below 0.5 Å the figure also shows the behaviour of spectrum as a function of λ, due to neutrons in moderation process. A real Maxwellian curve was calculated taking the λ exponent equal

to 5 instead 4.61, and is also plotted in the figure.

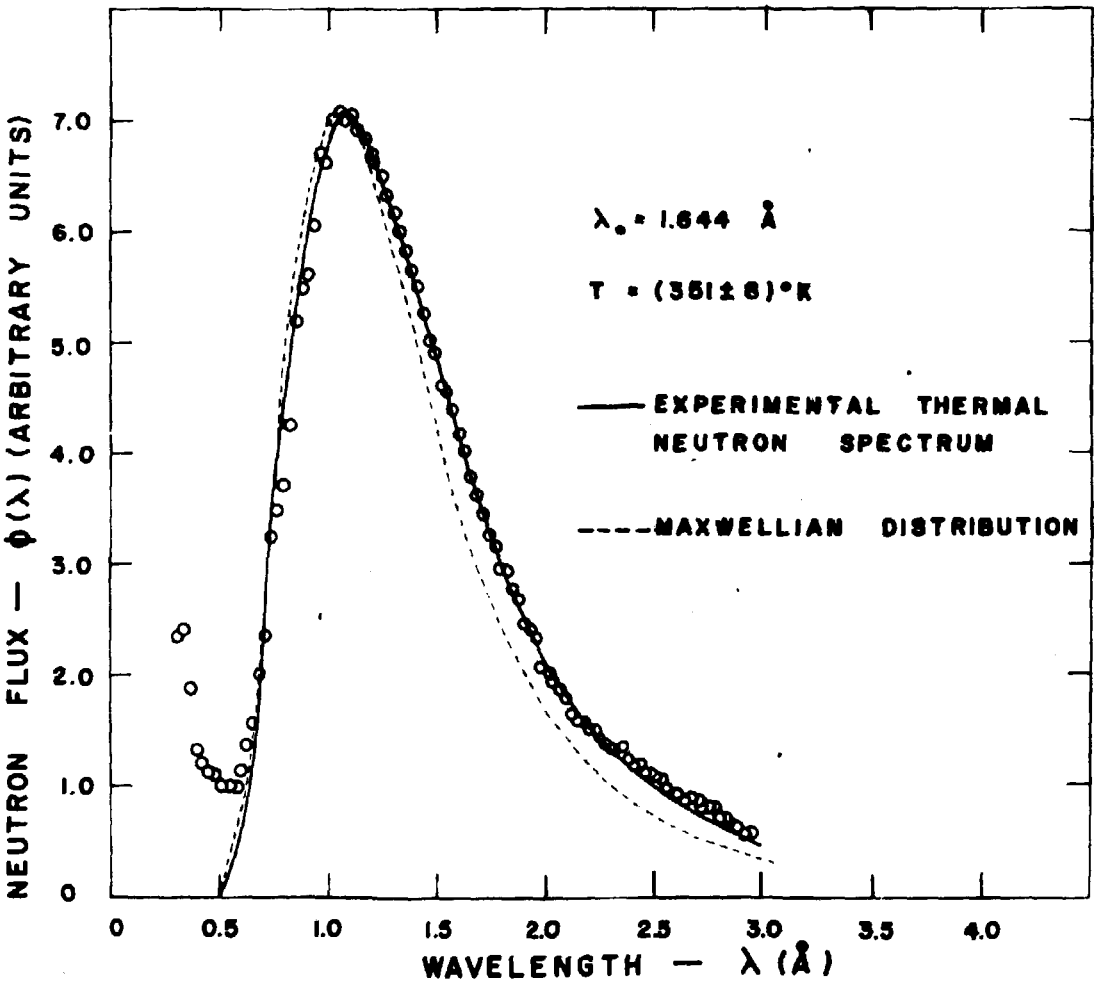

Figure 8 - Thermal Neutron spectrum emerging from the beam hole nº 10 of the IEA-R1 reactor

The chief utility of figure 8 is to describe the spectrum available for experimental use at the BH-10 beam tube facility; from the figure one can note that the experimental spectrum shape does not differs drasticlly from a real Maxwellian. Thus, to the spectral distribution given by eq. (25), an effective temperature can be associated. Experimental uncertainty in the count rate data leads to an estimated maximum uncertainty of 0.02 Å in the most probable wavelength; to the value $\lambda_o = 1.644 \pm 0.02$ Å corresponds the 351 ± 8°K effective temperature.

The Germanium crystal reflectivity calculation were previously made for the (111) planes[12,14]. However, in the calculation the used effective absorption coefficient was total macroscopic cross section of the element instead the crystal total cross section (fig. 2). Nevertheless, Jones concludes in his work[22] that when the reflectivity calculation is made by this procedure, the obtained spectral distribution presents a temperature not much different from the moderator temperature and this does not occur in the practice because of the previously exposed reasons.

The average moderator temperature of the IEA reactor is 306°K; the difference of 45°K between the temperatures agrees with the differences obtained from measurements carried out in other reactors[19,22,23].

The present work value of the effective temperature is in agreement with the value (T = 357 ± 8°K) obtained from spectrum measurement in other IEA reactor beam hole, using the IEA time do flight spectrometer[24].

RESUMO

O espectro de nêutrons térmicos do reator IEA-R1 foi medido no intervalo de comprimentos de onda de 0,3 Å a 3,0 Å, utilizando-se um espectrômetro de cristal. Um cristal único de Germânio, em reflexão, foi usado como monocromador, escolhido por serem teòricamente proibidas as reflexões de segunda ordem de seus planos (111).

A refletividade do cristal de Germânio utilizada na análise dos resultados foi calculada para as cinco primeiras reflexões permitidas. Nos cálculos foi usado um coeficiente efetivo de absorção do cristal, em vez da secção de choque macroscópica do elemento, que havia sido empregada nos cálculos de outros autores.

A razão de contagem do espectro medido foi corrigida para contaminações de ordens superiores e reflexões parasitas e processada de maneira a obter-se o espectro real de nêutrons térmicos em função do comprimento de onda.

Uma equação de tipo Maxwelliano, mas de expoente variável, foi ajustada por mínimos quadrados aos pontos experimentais entre 0,7 Å e 2,9 Å. Os resultados experimentais são também comparados com uma distribuição Maxwelliana teórica, resultando uma temperatura efetiva de 351 ± 8°K para os nêutrons, 45°K acima da temperatura média de 306°K do moderador.

RÉSUMÉ

Le spectre de neutrons thermiques du réacteur IEA-R1 a été mesuré dans une intervalle de longueurs d'onde entre 0.3 Å et 3.0 Å, en employant un spectromètre à cristal. Un monocristal de Germanium en réflection a été utilisé comme monochromateur, choisi parce que ses reflections de deuxième ordre sont théoriquement interdites pour les plans (111).

La réflectivité du cristal de Germanium utilisée dans l'analyse des résultats a été calculée pour les cinq premières réflections possibles. Pour les calculs, un coefficient effectif d'absorption du cristal a été utilisé, au contraire de la section efficace macroscopique de l'élément qui a été employé dans les calculs d'autres auteurs.

Les courbes de la raison de comptage du spectre mesuré ont été corrigées quant à la contamination d'ordres supérieurs et reflections parasites, et ont été traitées afin d'obtenir l'allure effective du spectre des neutrons thermiques en fonction de la longueur d'onde.

Une equation de type Maxwellien avec exposant variable, a été ajustée pour minimes carrés aux points expérimentaux entre 0.7 Å et 2.9 Å. Une comparaison entre les résultats expérimentaux et une distribution Maxwellienne théorique a été effectuée, en résultant une température neutronique effective de 351 ± 8°K, qui est 45°K audessus de la température moyenne 306°K du modérateur.

REFERENCES

1. Hughes, D.J., Pile Neutron Research, Addison Wesley Publishing Company (1953).

2. Leme, M.P.T., M.S.thesis, Escola Politécnica da Universidade de São Paulo, Brasil (1970).

3. Zinn, W J., Phys. Rev. 71, 752 (1947).

4. Borst, L.B. and Sailor, V.L., Rev.Sci.Instr. 24, 141 (1953).

5. James, R.W., "The Optical Principles of the Diffraction of X-Rays" (G.Bell and Sons, Ltd., London 1958).

6. Dietrich, O.W. and Als-Nielsen, J., Acta Cryst. 18, 184 (1965).

7. Bacon, G.E. and Lowde, R.D., Acta Cryst. 1, 303 (1948).

8. Holm, M.W., Phillips Petroleum Cie., Rep. IDO 16115 (1955).

9. Sailor, V.L. Foote, H.L., Landon, H.H., and Wood, R.E., Rev. Sci. Instr. 27, 26 (1956).

10. Weinstock, R., Phys. Rev. 65, 1 (1944).

11. Blake, F.C., Rev. Mod. Phys., 5, 169 (1933).

12. Brücker, B., Atomkernenergie 11, 381 (1966).

13. Fulfaro, R., Report IEA to be published.

14. Wajima, J.T., Rustad, B.M. and Melkonian, E., Jour.Phys.Soc. Japan 15, 630 (1960).

15. Popovici, M., Gheorghiu, Z. and Gelberg, D., Institute for Atomic Physics, Bucharest, Romania, FN-34 (1968).

16. Bacon, G.E., Neutron Diffraction, 2nd edition, Oxford University Press (1962).

17. Fowler, I.L. and Tunnicliffe, P.R., Rev. Sci. Instr. 21, 734 (1950).

18. Safford, G.T., Taylor, T.I., Rustad, B.M. and Havens Jr., W. W., Phys. Rev. 119, 1291 (1960).

19. Domeneci, M., Zucca, T., Rapporto SORIN 44 (1964).

20. Blinowski, K. and Sosnowski, J., Nucl. Instr. Methods 10, 289 (1961).

21. O'Connor, D.A. and Sosnowski, J., Acta Cryst., 14, 292 (1961).

22. Jones, Ian R., Lawrence Radiation Laboratory(Livermore) Rept. UCRL-7611, December (1963).

23. Holmryd, S., Sköld, K., Pilcher, E. and Larsson, K.E., Nucl. Instr. and Methods, 27, 61 (1964).

24. Vinhas, L.A., Ph.D. thesis, Universidade Estadual de Campinas, Brasil (1970).